FE ANALYSIS OF CLOSED CELL ALUMINUM FOAM UNDER IMPACT LOADING

[1]Christos Tegos, [1]Emanouil Smyrnaios, [1]Fani Stergioudi, [2]Georgios Maliaris, [1]Nikolaos Michailidis*

[1]Physical Metallurgy Laboratory, Aristotle University of Thessaloniki, Greece
[2]Additive Manufacturing Laboratory, International Hellenic University, Greece

KEYWORDS –

Closed-cell aluminium foams, Voronoi algorithm, Deshpande-Fleck model, Finite element method, Impact test

ABSTRACT –

Metal foams have been intensively explored for possible application in many industry domains like automotive, naval, aerospace and bioengineering due to superior mechanical energy absorption combined with their lightweight design. The mechanical behaviour of metal foams that are subjected to impact loads is still challenging and engineering application of these materials typically requires time-consuming experimental tests. As a result, numerous numerical models have been developed using the finite element method (FEM).

In this work, FEM models were built that explain the acting mechanisms that take place during impact, study the yield properties as well as the energy absorption during the impact of closed-cell aluminium foams. The simulation results are compared with the ones derived from respective experimental uniaxial tests. Two different modelling approaches were applied thus creating two models. The first model relies on a cell-based method where the initial geometry of the foam was generated based on the Voronoi tessellation algorithm. The generation of the solid elements for this model was optimized using automated tools of advanced pre-processor ANSA software package by setting appropriate mesh parameters and quality criteria in order to keep the exact shape of cells. The second one relies on the isotropic, strain-hardening, and continuum based model developed by Deshpande-Fleck. The FE results were visualized and processed in META post-processor. The explicit solver LS-DYNA was used for both finite element models.

TECHNICAL PAPER -

1. INTRODUCTION

Aluminum foams are widely applied in many industry domains like aerospace (1), naval (2) and automotive (3) due to superior energy absorption (4),(5) combined with their lightweight design. Moreover, their use is accompanied by efficient vibration damping as well as sound absorption capabilities (6),(7),(8). Hence, the study of aluminum foams in compression under high impact loading is essential for the determination of their mechanical behaviour.

In a quasi-static compression test, the basic influence factors are the base material properties, relative density and geometrical characteristics (9). However, in a high speed impact experiment, even if nominal stress-strain relationship is used to characterize the analysis like in a quasi-static test, other phenomena take place as well. Specifically, the strain-rate sensitivity of base material, trapped gas and micro-inertia effects are also considered as major influence factors (5), (9), (10), (11) making the study of metal foams under impact loading more complex. Moreover, the macroscopic strain-rate behaviour experienced by the metal foam is significantly different from the respective microscopic

strain-rate of the base material, due to localized large deformation even in the elastic region of metal foam.

Many researchers have turned to numerical simulations in order to gain inside the microscopic mechanisms and to characterize the bulk properties of foams. Two main model categories are widely used a) cell based models where the base material and internal gas are considered as different materials and b) continuum mechanics models where mechanical behavior of the foam material is modeled as a continuous mass since deformation and force experienced by the cells can be treated in a continuum sense. In this paper, two respective finite models were generated following the aforementioned two approaches: a cell based model generated according to Voronoi tessellation technique and the continuum-based model developed by Deshpande and Fleck.

The generation of a cell based model, using the Voronoi algorithm (12) in order to represent a cellular structure by evaluating specific parameters of the model compared to respective ones of the foam specimen, e.g foam porosity, pore ratio, mean pore size distribution, cell area and circularity in 3d space, is the most common practice (13), (14), (15). In case that those parameters are close to the real structure, the Voronoi model can depict the random and complex structure of a cellular structure quite satisfactory as well as perform well in terms of simulation efficiency (15), (16). In the present study, the generated 3D polyhedral by Voronoi algorithm were converted into closed-cell porous microstructures, considering also the ellipsoidal-like shape of the cells of the actual aluminum foam (15). Subsequently, the final produced geometry is the input in order to create a 3D finite element model consisted of solid elements.

The basic characteristic of a continuum-based model is a constitutive stress-strain relation. Several yield functions were proposed by researchers in order to try to describe the constitutive behavior of metal foams under complex loading. The model proposed by Deshpande and Fleck (namely D&F model) has been studied in detail and is used in this study (17).

2. FOAM MATERIAL AND IMPACT TEST

2.1. Foam Material

The samples used to conduct the experiments were extracted from a commercially available plate. They were cut by wire Electrical Discharge Machining (wEDM) in cylindrical shape with diameter d = 20 mm and height h = 30 mm. The porosity of the samples was measured 80% ± 1%. In order to characterize their microstructure, energy dispersive spectroscopy (EDS) as well as X-ray diffraction analysis (XRD) were performed, Figure 1a.
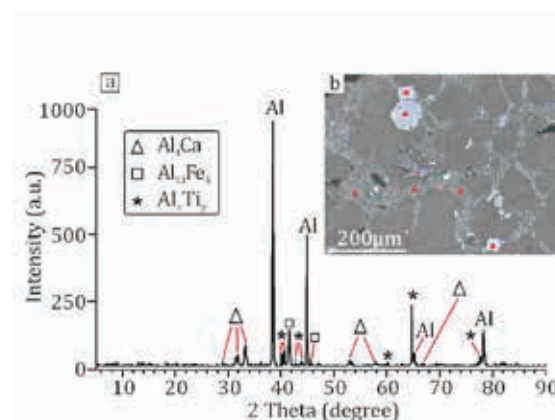

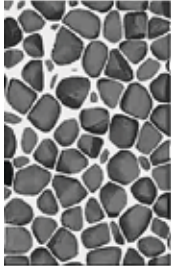Figure 1 – (a) Identified phases from XRD analysis. (b) Sample image from optical microscope

Different phases of aluminum were identified as a result of production process of the foam. Aluminum reacts with Al_4Ca phase and produces eutectic structure (laminate morphology), as shown in the optical microscope, <u>Figure 1b</u>. The white regions correspond to the Al_3Fe_4 phase, while the gray areas to Al_xTi_y.

<u>2.2. Impact Test</u>

Impact compression tests were performed on an impact tester apparatus fabricated in order to carry out dynamic load tests (15), according to the description of ISO 17340 (18). The impact velocity of the striker was measured by an accelerometer as well as a high speed camera, while the force was measured by a piezocrystal. Signals' noise was removed using the low pass filtering CFC600 (18). The experimental impact velocity was set at 7 m/s.

3. GEOMETRY GENERATION

The Voronoi foam geometry was realized using the Rhino software in combination with the Grasshopper add-on, a visual programming environment that allows building shape generators using generative algorithms (15). A cylinder with a diameter of 20 mm and height of 30 mm was obtained in order to match the dimensions of the Al-foam specimen used in impact experiments. <u>Figure 2</u> shows the results of the geometric features as well as the shape for both Voronoi and real geometry. The main differences are found in cell area and pore size since a higher percentage of microporous is present in real geometry, a characteristic feature that could not be produced by Voronoi algorithm.

Voronoi Geometry	Al Foam Geometry	Evaluation Parameters	Voronoi Geometry	Al Foam Geometry
		Porosity	80 %	80 ±1%
		Cell area	3,65 mm	2.96 mm
		Pore size	6.2 mm	4.74 mm
		Circularity	0.69	0.72
		Pore ratio	1.7	1.54

10 mm 10 mm

Figure 2 - Evaluation parameters of Voronoi and real foam geometry

4. FE MODELLING

<u>4.1 Voronoi Model</u>

First order, tetrahedral elements were selected for the Voronoi geometry. The total number of generated elements was 217200, the selected element formulation one-point nodal pressure tetrahedrons and the average element length was ~0.48 mm. The generation of the solid elements was optimized using automated tools of advanced pre-processor ANSA software package by setting appropriate mesh parameters and quality criteria in order to keep the exact shape of cells (19). LS-DYNA explicit solver was used for the solution of FE model (20).

A rigid plate was created, consisted of shell elements with a total weight 850 g which crashes into the sample with velocity of 7m/s, similar to the experiment. Fixed zero displacement were imposed on the nodes at the bottom of the sample along x,y, and z axes and also zero rotation with respect to the same axes. Contact of type surface-surface was defined between the plate and the sample. The coefficients of friction, static and dynamic, were determined at μs = 0.3 and μD = 0.23 respectively. Contact was also defined between the elements of the

foam itself with a static coefficient of friction μs = 0.18. The type was single surface. Figure 3 shows the final meshed model with the applied boundary conditions.
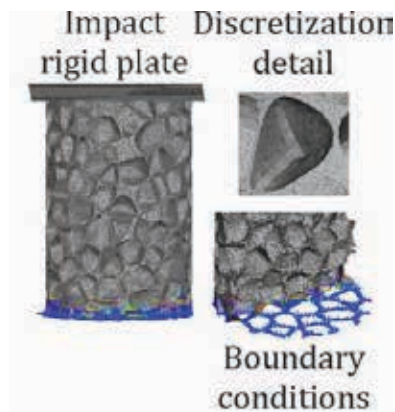

Figure 3 - The developed FE model for simulating the impact response of aluminum foam

The material selected was pure aluminum with Young's modulus E = 69 GPa, Poison ratio v = 0.33 and density ρ = 2.7 Kg/cm^3. The corresponding elasto-plastic LS-DYNA material, MAT PIECEWISE LINEAR PLASTICITY was selected in order to describe the plastic area. In addition, a nonlinear material law was applied, depending on the rate of deformation as shown in Figure 4.
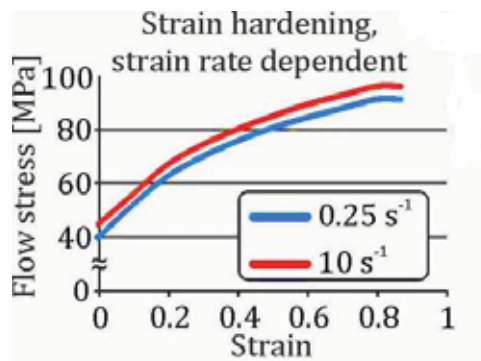

Figure 4 – Stress-strain curves of base aluminum used for the simulation

In order to simulate the collapse of the cells under impact loading due to high plastic strain values, the element erosion method was used so that highly distorted elements are removed. In order to achieve this, different Strain Fail Criterion (SFC) was set and respective solutions were performed. Specifically, strain values of 0.5, 0.6, 0.7, 0.8 and 0.9 were defined. At the time when one element reaches the SFC, is removed from the structure. In practice, this means that the porosity increases as much as the percentage of data that fails at each time step. Figure 5 shows the percentage of elements that failed, in terms of displacement for each SFC. It is clear that the increase of the SFC increases the number of failed elements, almost linearly to displacement. Most of the failed elements are located at the thin beams of the structure, which is in line with the experimental observations. Finally, the SFC of 0.8 was selected, which actually represents the local breaks of the structure during impact. The selected SFC value is greater than the respective strain value that corresponds to UTS of aluminum. The reason is that in experiment even if the base material exceeds UTS in some cases, remains to foam structure. In contrary, the failed elements are directly removed from the structure as the simulation continues.
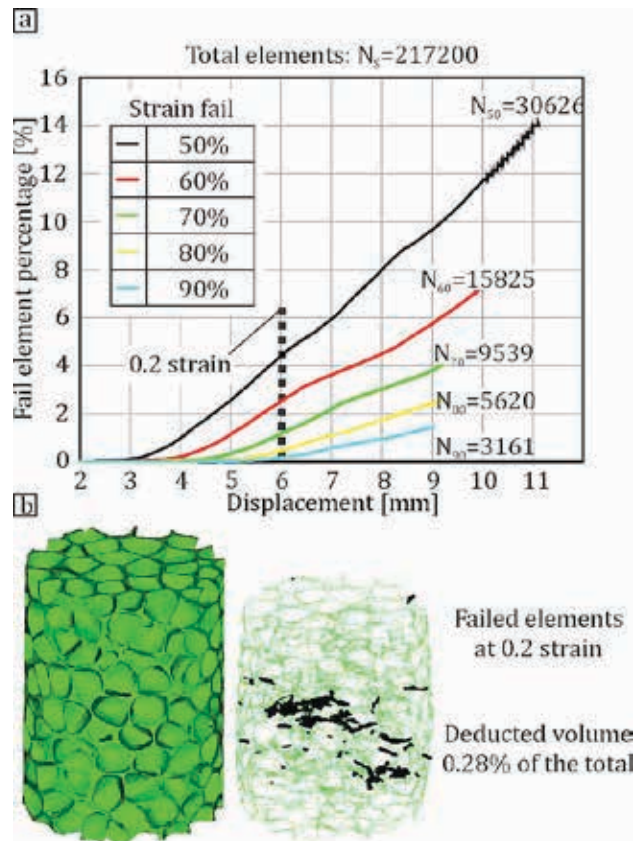
Figure 5 - a) Failed element percentage and number according to element SFC. b) Failed element distribution at the plateau region (strain 0.2) using 80% SFC

4.2 Deshpande and Fleck Model

The Deshpande and Fleck model takes into account the effect of hydrostatic pressure on yielding based on the von Mises effective stress σ_e and the mean stress σ_m and is described by a yield surface of elliptical shape in $\sigma_m - \sigma_e$ plane (17), (21).

Equation (1) describes the yield surface of Deshpande and Fleck model (17).

$$\Phi = \hat{\sigma} - Y = \sqrt{\frac{1}{\left[1+\left(\frac{\alpha}{3}\right)^2\right]}\left[\sigma_e^2 + \alpha^2\sigma_m^2\right]} - Y \quad (1)$$

where Φ is the yield function, Y the yield strength and $\hat{\sigma}$ the equivalent stress. Parameter α is the shape factor that defines the aspect ratio of the ellipse and is related to the plastic Poisson's ratio v_{pl}, which can be determined by:

$$\alpha = 3\left(\frac{0.5-v_{pl}}{1+v_{pl}}\right)^{\frac{1}{2}} \quad (2)$$

In contrary to tetrahedrons used in Voronoi model, first order hexahedral elements were selected. The element formulation was one-point corotational as suggested for foam structures (20) and the total number of elements: 78780. Same boundary conditions as in Voronoi model were applied. A similar contact was defined between the rigid plate and foam. Although it is a continuum model, an interior contact was also applied to hexahedral elements themselves in order to avoid negative volumes and error terminations during solution since high pressure values are developed (20). The constituve Deshpande and Fleck model has been implemented in LS-DYNA taking into account strain hardening effects

and the variation of foam density per element (22). The yield stress function can be formulated as:

$$Y = \sigma_p + \gamma \frac{\hat{\varepsilon}}{\varepsilon_D} + \alpha_2 \ln\left(\frac{1}{1-\left(\frac{\hat{\varepsilon}}{\varepsilon_D}\right)^\beta}\right) \quad (3)$$

Materials parameters: plateau stress σ_p, γ, α_2, β can be obtained from the stress–strain data of the uniaxial impact test by fitting them to a curve described by equation (3). Figure 6 illustrates the experimental stress strain data and the curve fit of the yield stress function, used to obtain the material parameters.
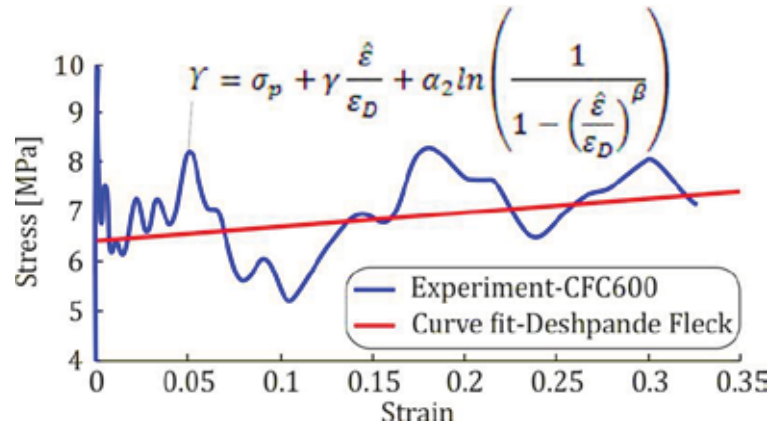

Figure 6 - Deshpande-Fleck yield function curve fit to experimental stress-strain data

Finally, the densification strain ε_D in equation (3) is defined as:

$$\varepsilon_D = -\frac{9+a^2}{3a^2} \ln\left(\frac{\rho_f}{\rho_{fo}}\right) \quad (4)$$

where a defines the shape of yield surface, equation (2). Plastic Poisson's ratio v_{pl} can be set equal to 0 in closed metal foams since it does not influence significantly the results (23), (24). All the parameters of Deshpande-Fleck material model are summarized in table 1.

E [MPa]	ρ [kg/mm^3]	α	γ [MPa]	ε_D	α_2 [MPa]	β	σ_p
1800	5.41e-7	2.12	4.58	1.61	46	5.3	6.4

Table 1 - Deshpande-Fleck parameters used for material model

Deshpande-Fleck model was much simpler in terms of geometry and therefore the time solution was only 45 minutes compared to ~12 hours of Voronoi model.

5. RESULTS AND DISCUSSION

FE results from both models were visualized, processed and compared with the experimental ones derived from uniaxial tests in META post-processor (25). The overall workflow is demonstrated in figure 7.
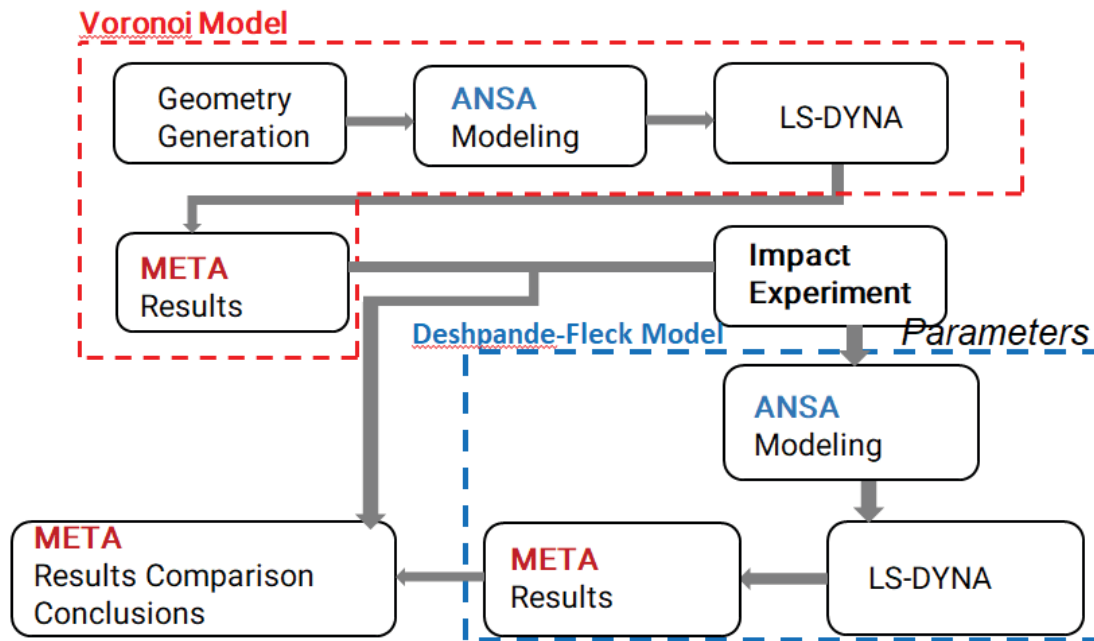
Figure 7: Workflow showing the generation, modeling, solution and post-processing of FE models

Stress - strain curve obtained by the force – displacement curve of the FE analysis as well as the experimental one are illustrated in figure 8b. The experimental curve of this figure represents the average evaluated by three experiments. There is a satisfied correlation of experimental results with those derived from FE analysis. In the linear region, the slope of both curves is quite similar. However, the plateau area of Voronoi model starts 2.6 MPa lower than the experimental one but they converge as the displacement increases and reach almost the same values at 0.2 strain.

This stress peak observed on the experiments can be explained in the presence of Al_3Fe_4 phase, which during loading induces a local stress increase around it. These local stress fields interact with the surrounding phases as deformation increases. Micro inertia phenomena also appear during material flow since the mass of the phase is different from that of the base aluminum (26). The above, reduces the mobility of Al_3Fe_4 phase leading to increased strength.

In order to analyze further this experimental stress peak, a new low energy experiment was performed, having a much lower initial velocity as input so that the elastic region is not exceeded, until strain ~ 0.025. At this strain value in the elastic region, fractures of the Al_3Fe_4 phase were identified using SEM, as shown in Figure 8a. The smaller dimension phase results to reduction of local stress fields, thus the mobility of Al_3Fe_4 phase becomes higher in the aluminum matrix leading to decrease of total strength as entering the plateau region. This observation can give the reason why the convergence of the FEM diagrams and experimental one (Figure 8b), is achieved at 0.2 strain. In conclusion, a considerable percentage of the impact energy is consumed for the fracture of Al_3Fe_4 phases. This percentage is estimated at 8% of the total deformation energy (shaded region Figure 8b).
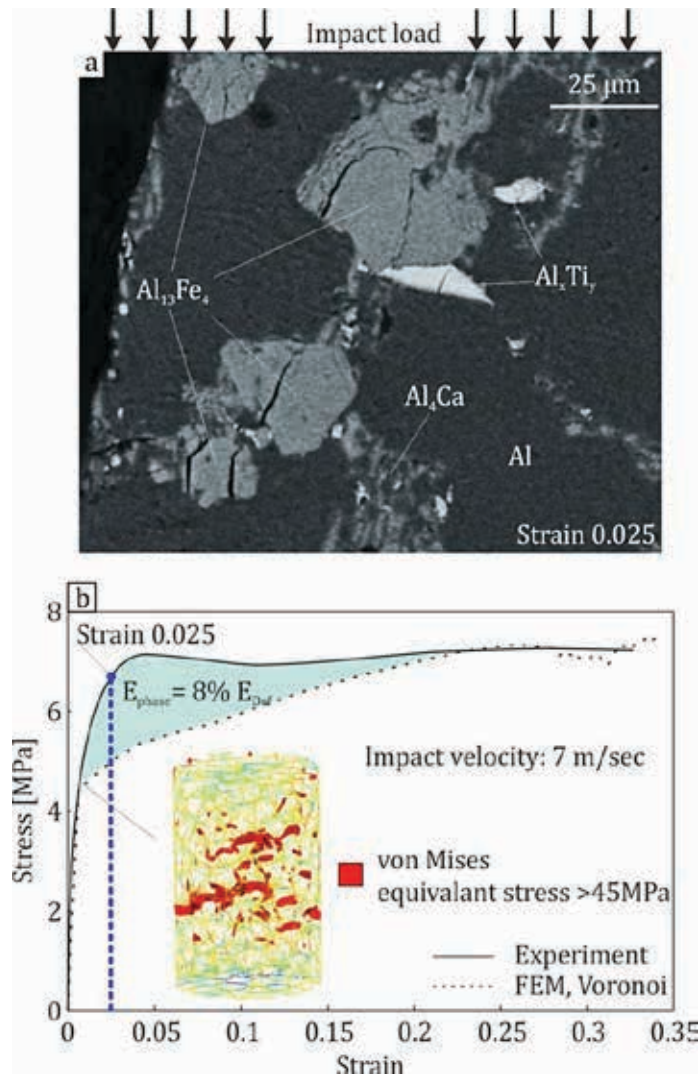
Figure 8 - a) SEM: micro-scale changes in the structure of sample after impact loading at the end of linear region. b) Stress-strain curve of experiment and Voronoi model

Furthermore, FE analysis revealed the development of high local stresses in linear region that exceed the yield stress of aluminum. Figure 8b demonstrates the distribution of local von Mises stress at the end of the linear region which exceeds 45 MPa. They are concentrated in the thin beams of Voronoi model, as expected.

Figure 9 shows the macroscopic forms of deformation for the impact experiment as well as Voronoi model at strain value of 0.025 and at strain value of 0.3.
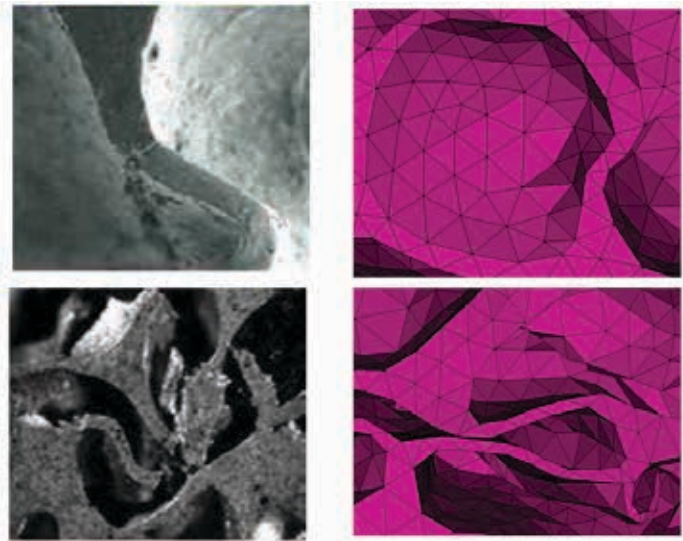
Figure 9 - Macroscopic forms of deformation of impact experiment and Voronoi model at 0.025 and 0.3 strain respectively.

Similar forms of deformation are observed. At the end of linear region (strain 0.025), the main deformation mechanism is the plastic buckling of cell walls whereas the total collapse and crushing of cells in plastic region (strain 0.3).

Finally, Figure 10 summarizes the derived stress-strain curves of both FE models, Voronoi and Deshpand-Fleck, as well as the average one determined by the experiments. As expected, since constitutive Deshpand Fleck model has as input experimental material parameters, is very close with the experiment, both in elastic and plastic region. The main differences were found between Voronoi model and experiment as explained in Figure 7b.

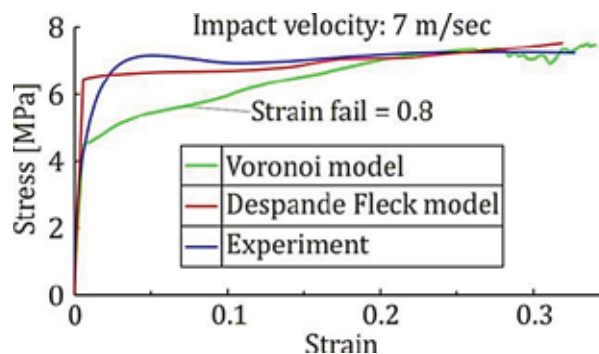Figure 10: Stress-strain curves of experiment, Voronoi and Deshpande-Fleck models

6. CONCLUSIONS

In this work, two FE models were generated in order to study the overall behavior of closed cell aluminum foam under impact loading. The first one was based on the Voronoi algorithm as approximation of the actual geometry. The results obtained by FE analysis are consistent with those obtained by the respective experiments.

Specifically, a satisfied convergence of stress-strain curve between Voronoi model and experiments was achieved. A significant difference was found at the end of linear area where the stress found in the experiments was ~20% greater than the one calculated on FE analysis. Then, the two curves converged as the deformation increases and entering the plateau region. This stress peak was explained by studying the microstructure of the sample. The Al_3Fe_4 phase contained in the foam structure was a reinforcing factor at the early stages

of deformation. Thus, a considerable percentage of the impact energy was consumed for the fracture of Al_3Fe_4 phase.

The deformation mechanisms that take place during the impact were also investigated. Similar deformation forms of Voronoi model and foam samples were found both in elastic and plastic region. Moreover, the Voronoi model was used in order to find the areas where the stress exceeds the yield point in elastic region and thus local plastic deformation occurs. As expected, these areas were mainly in the thin beams of the cells. For all the aforementioned reasons, the FE model generated by the Voronoi algorithm can be used to characterize mechanical properties of aluminum foam.

The isotropic, hardening FE model, developed by Deshpande and Fleck was also examined. The derived stress-strain curve was very close with the experimental one. The main advantage was the simplicity of the model in terms of pre-processing and solution compared to Voronoi model.

REFERENCES

(1) 2. Amol A. Gokhale, N. Eswara Prasad, Biswajit Basu. Light weighting for defense, aerospace, and transportation. Springer Nature. 2019

(2) Crupi V, Epasto G, Guglielmino. Comparison of aluminium sandwiches for lightweight ship structures: honeycomb vs foam. Marine Structures. 30, 2013, pp. 74-96.

(3) Xiao Z, Fang J, Sun G, Li Q. Crashworthiness design for functionally graded foam-filled bumper beam. Advances in Engineering Software. 85, 2015, pp. 81-95.

(4) Gibson LJ, Ashby MF, Zhang J, Triantafillou TC. Failure surfaces for cellular materials under multiaxial loads—I Modelling. International Journal of Mechanical Sciences. 31, 1989, pp. 635-663

(5) Gibson LJ, Ashby MF. Cellular solids: Structure and Properties. Cambridge University Press. 2, 1997

(6) P.S. Liu, G.F. Chen. Application of Porous Metals. Porous Materials, Processing and Applications. 2014

(7) Schaeffler, R. A new generation of materials and their production methods. Advanced Engineering Materials. 8, 2006, pp. 773-777

(8) Seeliger, H.-W. Aluminium Foam Sandwich (AFS) Ready for Market Introduction. Advanced Engineering Materials. 6, 2004, pp. 448-451

(9) C.R. Calladine, R.W. English. Strain-rate and inertia effects in the collapse of two types of energy-absorbing structure. International Journal of Mechanical Sciences. 26, 1984, pp. 689-701

(10) B. Hou, H. Zhao, S. Pattofatto, J.G. Liu, Y.L. Li. Inertia effects on the progressive crushing of aluminium honeycombs under impact loading. International Journal of Solids and Structures. 26, 2012, pp. 2754-2762

(11) P.J. Tan, S.R. Reid, J.J. Harrigan, Z. Zou, S. Li. Dynamic compressive strength properties of aluminium foams. Part I—experimental data and observations. Journal of the Mechanics and Physics of Solids. 53, 2005, pp. 2174-2205

(12) Voronoi, G. F. Nouvelles applications des paramètres continus à la théorie des formes quadratiques. J. reine angew. Math. 134, 1908, σσ. 198-287

(13) Y. W. Kwon, R. E. Cooke, C. Park,. Representative unit-cell models for open-cell metal foams with or without elastic filler. Materials Science and Engineering A. 343, 2003, pp. 63-70

(14) G. Frenkel, R. Blumenfeld, P. R. King, M. J. Blunt. Topological Analysis of Foams and Tetrahedral Structures. Advanced Engineering Materials. 11, 2009, pp. 169-176

(15) N. Michailidis, E. Smyrnaios, G. Maliaris, F. Stergioudi, A. Tsouknidas. Mechanical Response and FEM Modeling of Porous Al under Static and Dynamic Loads. Advanced Engineering Materials. 2014, pp. 289-294

(16) Xiaoyang Zhang, Liqun Tang, Zejia Liu, Zhenyu Jiang, Yiping Liu, Yidong Wu. Yield properties of closed-cell aluminum foam under triaxial loadings by a 3D Voronoi model. Mechanics of Materials. 104, 2017, pp. 73-84

(17) V.S. Deshpande, N.A. Fleck. Isotropic constitutive models for metallic foams. Journal of the Mechanics and Physics of Solids. 48, 2000, pp. 1253–1283

(18) Metallic materials-Ductile testing-High speed compression test for porous and cellular metal. s.l. : International Organization for Standardization, 2014. ISO 17340

(19) ANSA, version 22.1.4, BETA CAE Systems. 2022

(20) LS-DYNA, version R11.2.0, Livermore Software Technology Corporation. 2021

(21) V.S Deshpande, N.A Fleck. Multi-axial yield of aluminium alloy foams. Materials Science. 1999

(22) Reyes A, Hopperstad OS, Berstad T, Langseth M. Implementation of a Material Model for Aluminium Foam in LS-DYNA. Department of Structural Engineering, Norwegian University of Science and Technology. 2002. Report R-01-02

(23) Hanssen AG, Hopperstad OS, Langseth M, Ilstad H. Validation of constitutive models applicable to aluminium foams. International Journal of Mechanical Sciences. 44, 2002, σσ. 359-406

(24). C. Zhu, Z. Zheng, S. Wang, K. Zhao, J. Yu. Modification and verification of the Deshpande-Fleck foam model: A variable ellipticity. International Journal of Mechanical Sciences. 151, 2018, σσ. 331-342

(25) META, version 22.1.4, BETA CAE Systems. 2022

(26) F. A. McClintock, A. S. Argon. Mechanical behavior of materials. s.l. : CBLS, 1999